GEOFYSISKE PUBLIKASJONER

GEOPHYSICA NORVEGICA

VOL. XXII NO. 4

MOTHER OF PEARL CLOUDS OVER SOUTHERN NORWAY, FEBRUARY 21, 1959

BY YNGVAR GOTAAS

FREMLAGT I VIDENSKAPS-AKADEMIETS MØTE DEN 9DE DESEMBER 1960 AV ELIASSEN

Summary. Beautiful mother of pearls clouds and cloudveils were observed over Southern Norway on February 21, 1959. Some 50 photos have been examined and height and location of the clouds determined. The clouds were situated at heights ranging from 20 to 27 km. They occured in a strong NW-ly airstream which had a maximum speed of 135 knots at 9 km. An observed cooling in the stratosphere is discussed and shown to be due mainly to large scale vertical motions. The additional cooling, necessary to cause condensation, can be explained by the cooling of the air at the crests of mountain waves.

1. Introduction. In the late evening February 21, mother of pearl clouds were observed over Southern Norway. Some 50 photos, mostly colour ones, were collected. Those taken simultaneously from different locations have been used to locate the clouds and to investigate their structure. The horizon is visible on the photos, so that angles are measured with an accuracy of approximately 0.05 degrees, by use of a theodolite and photos of a fixed grid.

2. Weather situation. Fig. 1 shows the surface chart 1500 GMT together with the 300 millibar chart at 1200 GMT, February 21. Showers occurred along the windward coastline and over the northern mountain districts. Over central and southern parts of Southern Norway only scattered stratocumulus clouds at times obscured the mother of pearl clouds.

Wind and temperature variations as observed by different radiosonde stations are shown in Fig. 2 and Fig. 3. From these observations and from upper air charts, curves are drawn showing wind and temperature distribution in the region where

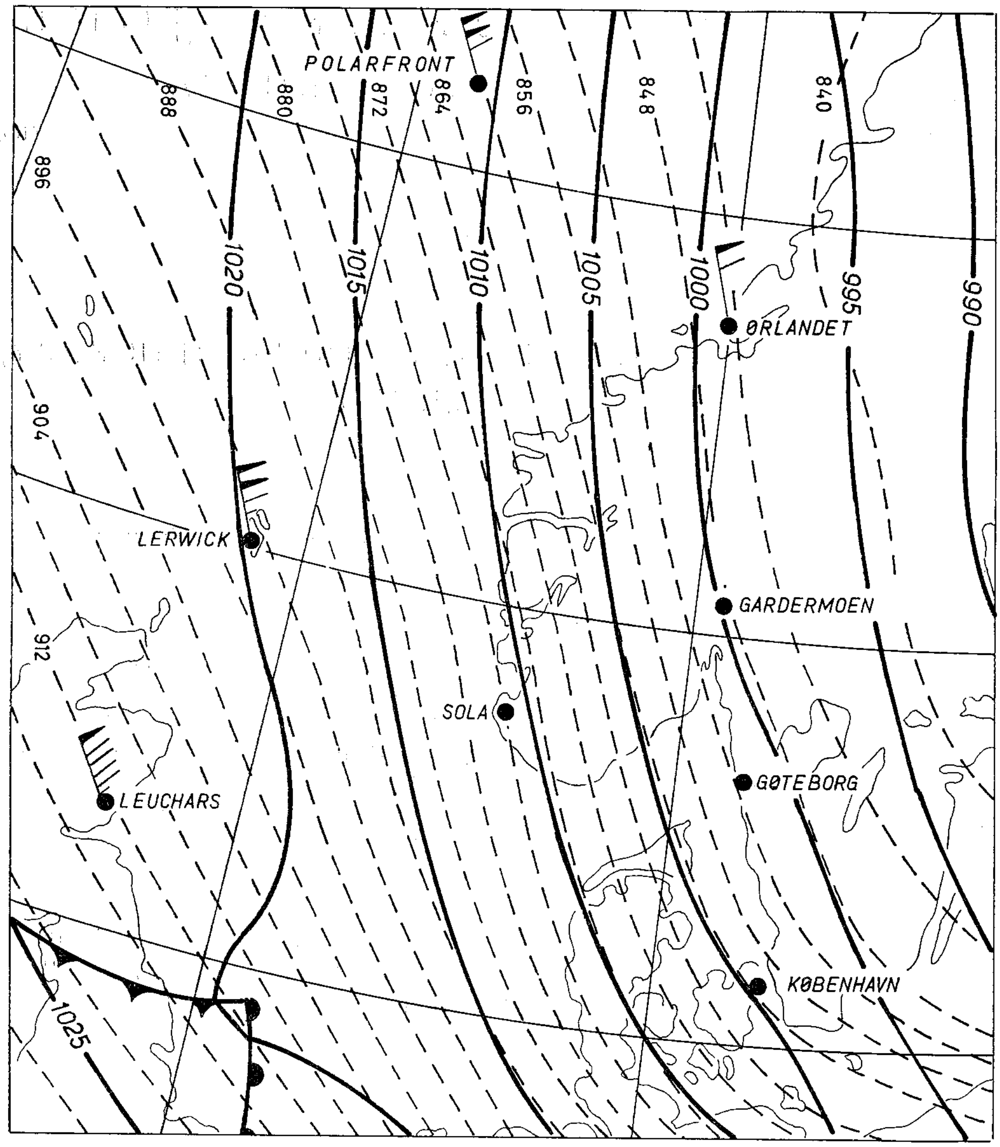

Fig. 1. Surface chart 1500 GMT and 300 millibar chart 1200 GMT, February 21, 1959. Heights in decameters.

the clouds were observed and at the time of their occurrence, 1530—1730 GMT. Regarding temperatures above 17 km there may be some doubt as to the curves drawn. The lowest temperature recorded, —82° C, was at 22 km over Ørlandet at 1200 GMT, February 21. The highest windspeed observed over Norway was 128 knots at 9 km over Gardermoen. Unfortunately the Sola ascents do not contain any wind records.

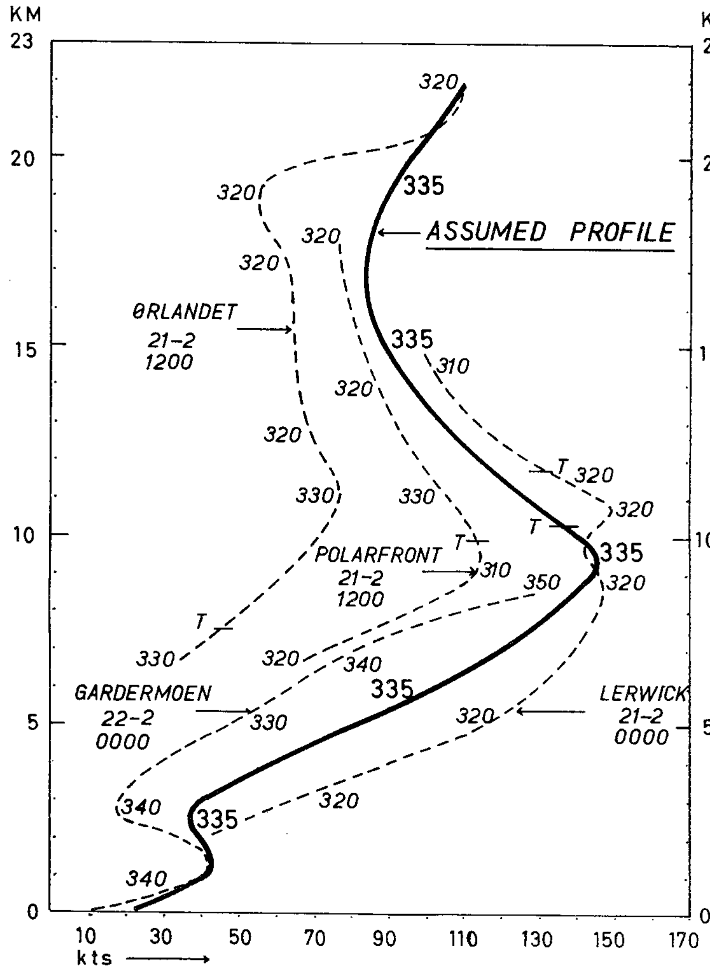

Fig. 2. Upper wind observations. Numbers show wind-directions in degrees. The solid curve shows the wind profile appropriate for the occurrence of mother of pearl clouds.

3. Location of clouds. The position of the clouds, the heights of which can be fairly accurately measured, are shown in Fig. 4. Photos taken from Holt, Drammen, Lier, Oslo, Lillestrøm and Stange were used. For the astronomical refraction average values were taken. The clouds shown in Fig. 4 were not all observed at the same time. The cloud, or rather sample of clouds, marked A was located by means of photos taken at 1615 GMT from Holt and Oslo. Later in the evening it was hidden by low clouds and no more photos could be taken. A thin bluish veil extended from the cloudmass in a SE-ly direction. Its position can only be approximately sketched. Of the other clouds several photos were taken in the period 15.43 to 17.30 GMT. In addition to the clouds shown in Fig. 4 many smaller clouds were visible at different times, rapidly

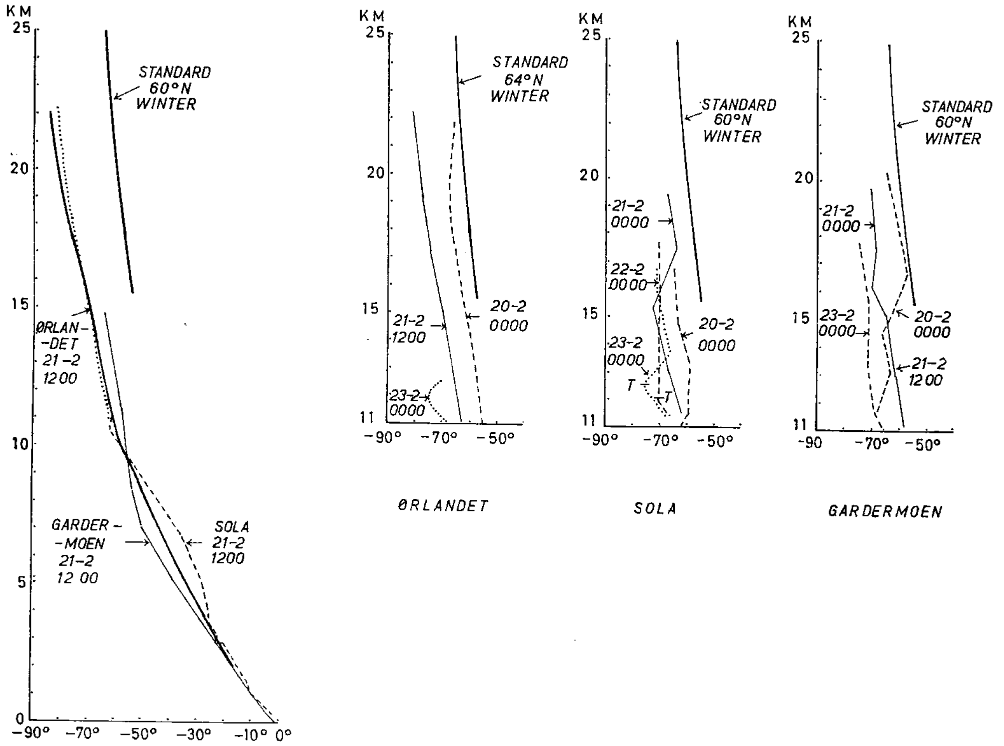

Fig. 3. Observed temperatures. The solid curve shows the assumed temperature profile appropriate for the occurrence of mother of pearl clouds. The values of standard temperatures are taken from MURGATROYD (4).

changing their sizes and structures. A movement of 2.5 km in one minute was observed of one of the edges. This indicates that caution must be used when examining photos which are not simultaneous. Apart from these apparent motions, the main body of the clouds were observed to be practically stationary. For 3 hours the cloud marked B was visible at the same spot, only varying in size and structure and shrinking with time. This cloud was the last to disappear, at around 17.30 GMT. Green-bluish veils also extended from the clouds B and E. These veils could be measured and located. Especially the clouds marked C and D rapidly changed their structures and only lasted for half an hour. Some of the photos are shown on page 15.

In the Figures 5—7 some of the measured heights and distances are shown.

4. Colour of clouds.

4.1 There seems to be a tendency, especially in the smaller clouds, for the colours to be arranged in bands along and parallel the borders, red colours dominating at the outer edges, green and blue colours towards the central parts of the clouds, the colours being correlated to the particle size. But often the mother of pearl cloud seems to be made up of a number of cloudsheets and cloudlayers rather than to appear as well as defined single cloud. This fact may contribute to the observed irregularity of colours in larger clouds as for instance is seen on the photo from Holt (photo 1). From this picture it is also clear that the arrangement of colours do not show any simple correlation with angular distance from the sun.

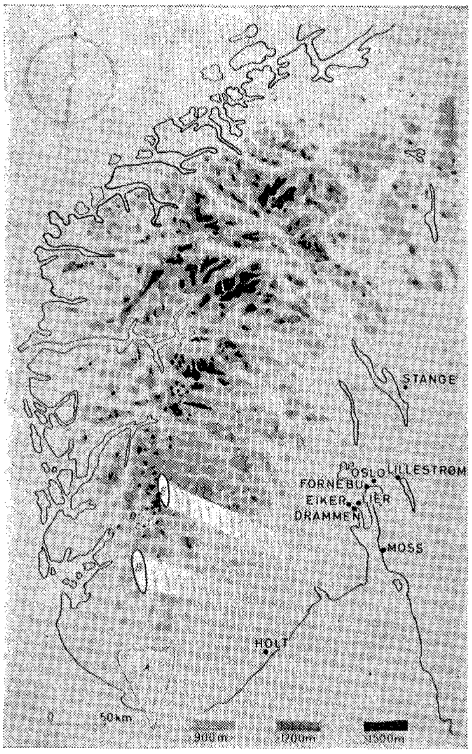

Fig. 4. Location of mother of pearl clouds, February 21, 1959.
Time of observations: 1520 – 1730 GMT.

The thin veils all have a very uniform green-bluish appearance. That may be due to scattering by particles smaller and of a more uniform size than those forming the clouds. In the early morning of February 22 a few clouds were visible from Oslo in a NW-ly direction. They then had a light grey-bluish appearance. Similar observations have previously been done and can be explained by backward scattering.

4.2 An interesting report on stratospheric clouds over Caucasus on the night September 13, 1953, has been given by DRIVING and SMIRNOVA [1]. The clouds were not visible, but showed on photos taken by use of a searchlight beam. They were located

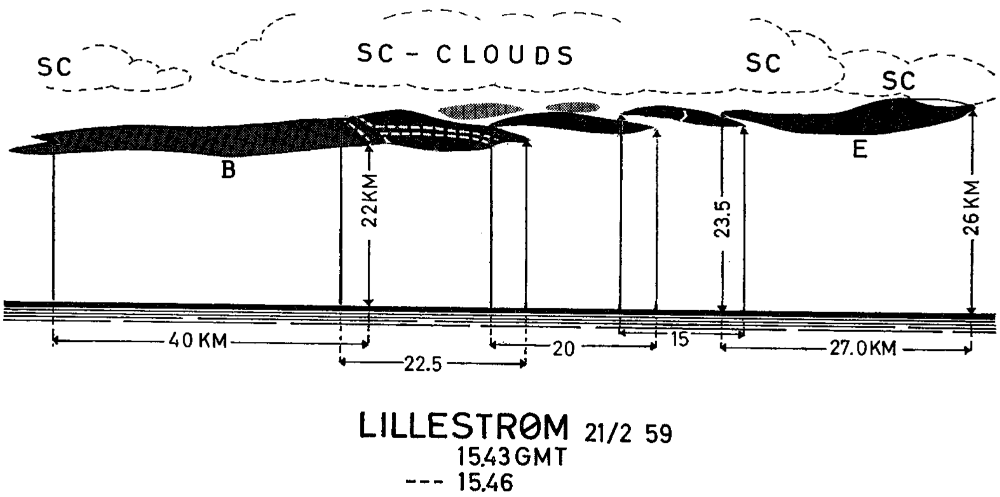

Fig. 5. Clouds as seen from Lillestrøm 1543 and 1546 GMT. Note the shrinking of cloud B in 3 minutes. Part of the veils, in this case resembling clouds, are seen at the top, but mostly the veils are hidden by stratocumulus clouds.

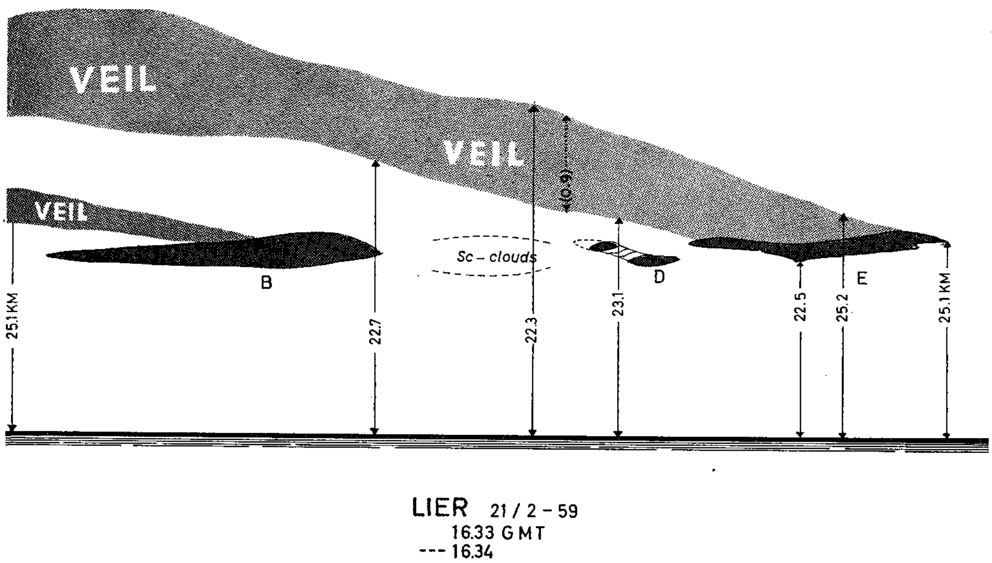

Fig. 6. Mother of pearl clouds seen from Lier 1633 and 1634 GMT. Cloud C is here hidden behind low stratocumulus clouds.

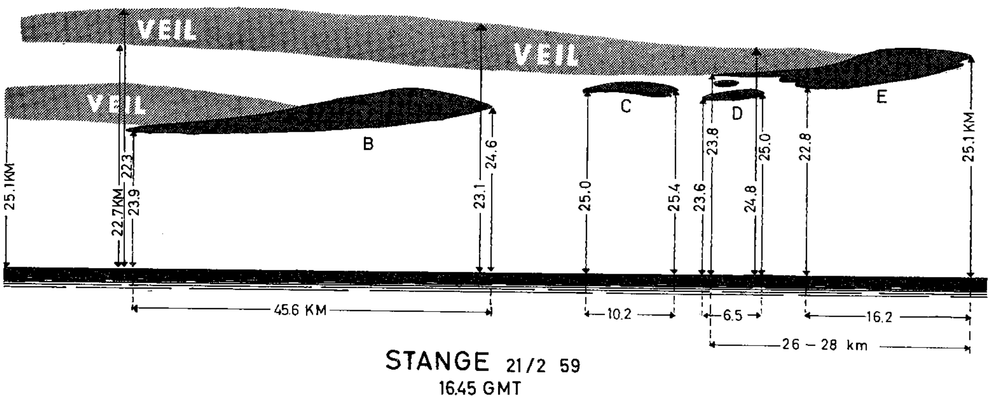

Fig. 7. Mother of pearl clouds seen from Stange 1645 GMT.

at heights between 21 and 24 km. Upon inspection of polarization curves it was found that the particles could not consist of ice, but were water droplets, the mean diameter of which was 0.7 microns. These clouds may have been of the same nature as the veils observed over Norway. The lifting of the air at the crests of mountain waves may have been so small that conditions were unfavourable for a further growth of the particles (Hesstvedt, [2]).

5. The formation of the clouds.

5.1 Hesstvedt [3] has shown that although the humidity in the stratosphere is very low, it is possible for condensation to occur provided the temperatures in the layers concerned drop to $-90°$ C. The mean temperature at 60 *N* in winter only reaches about $-65°$ C at heights between 20 and 30 km. The value of standard temperatures is taken after Murgatroyd [4]. As one can see from Fig. 3 the temperatures on February 21 were far below normal values. Above or below this height interval mother of pearl clouds are generally not observed, the temperatures being too high. As regards humidity one fact may be of importance. When NW-ly winds prevail over Norway in winter, the radiosonde ascents are of the polar winter type. There is no sharp inversion at the tropopause level and even isothermal layers may not exist. In Fig. 3 the temperature continues to fall into the stratosphere. The possibility exists that with a practically lacking tropopause the humidity can more freely be transported from the troposphere into the stratosphere, thus giving dew point temperatures somewhat above normal values in the layers concerned. Even slightly higher values will raise the temperature necessary to cause condensation considerably.

5.2 The local cooling of the air necessary for condensation may partly be explained by the lifting of the air at the crests of mountains waves. But another cooling process must take place to explain the abnormal low temperatures observed in the stratosphere over a larger region on February 21. Over Ørlandet (Fig. 3) the temperature at 22 km dropped 15° C from 0000 GMT February 20, to 1200 GMT February 21. Unfortunately only a few radiosonde ascents reach such heights as to permit the drawing of reliable upper air charts covering larger areas, at levels corresponding to the heights where the mother of pearl clouds were observed. Anyway, a 50 millibar chart has been constructed based on the few observations available. It is shown in Fig. 8. The remarkably low temperatures over Southern Norway are clearly shown, and can hardly be explained by advection alone. Vertical motions must play an important part.

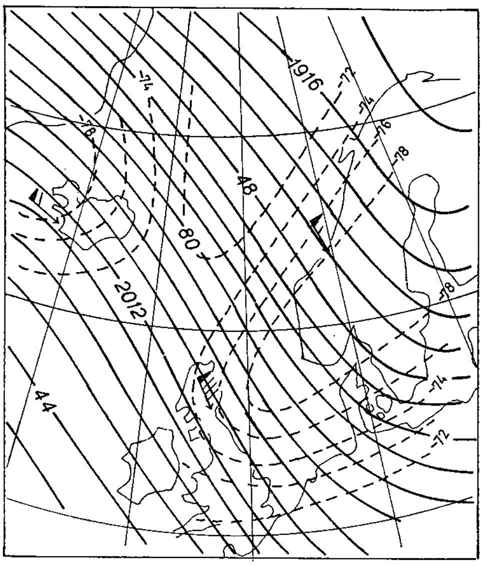

Fig. 8. 50 millibar chart, 1200 GMT, February 21, 1959. The solid lines show heights in decameters. Dashed lines show temperature in centigrades.

5.3 To get an idea of the nature of the large scale vertical motions we may consider the hydrodynamic equations. Assuming that at every instant the distribution of temperature and vorticity is in agreement with the thermal wind equation, the equation for vertical motion, with pressure, p, as vertical coordinate, can be written [5]:

$$-\frac{\alpha}{\theta}\frac{\partial\theta}{\partial p}\nabla_p^2\,\omega + \lambda^2\frac{\partial^2\omega}{\partial p^2} = \lambda\frac{\partial}{\partial p}\left[\boldsymbol{v}_g\cdot\nabla_p(\lambda+\zeta_g)\right] + \nabla_p^2\left[\boldsymbol{v}_g\cdot\nabla_p\,\alpha\right]$$

We have here neglected the influence of friction and heat sources.

α = specific volume, θ = potential temperature, $\omega = \frac{Dp}{dt}$ formally takes the role of the vertical velocity, λ = vertical component of the Coriolis parameter, $\boldsymbol{v}_g$ = geostrophic wind and ζ_g = relative vorticity (geostrophic). For the purpose of qualitative discussion we may as a first crude approximation replace the left hand side by $-C\omega$, where C is a positive coefficient. Neglecting deformation terms, the right hand side can be approximated by the term $2\lambda \frac{\partial \boldsymbol{v}_g}{\partial p} \cdot \nabla_p \zeta_g$. The vertical notion is then controlled by the advection of absolute vorticity by the thermal wind. Neglecting the variation of the Coriolis parameter we see that ascending motion is found in regions where the thermal wind blows from high to low vorticity [6].

In Fig. 9 thickness lines are drawn as the difference between the 50 millibar and

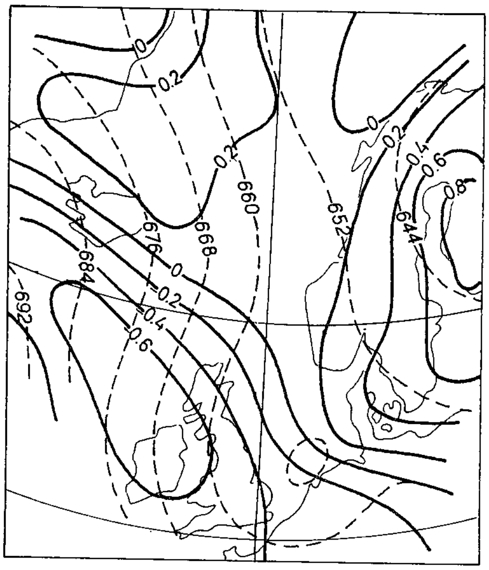

Fig. 9. Thickness 50/150 millibar, 1200 GMT, February 21, 1959, shown as dashed lines. Unit: decameter. Solid lines show the distribution of absolute vorticity (geostrophic). Unit: 10^{-4} sec^{-1}.

150 millibar levels. Further is shown the distribution of absolute geostrophic vorticity at the 100 millibar level. The geostrophic vorticity $\zeta_g = \frac{g}{\lambda} \nabla_p^2 \mathcal{Z}$, where $\mathcal{Z}$ is absolute height and g the accelleration of gravity, has been computed from the readings of $\mathcal{Z}$ in a centerpoint and 4 surrounding points. The distance from the centerpoints is here 300 km. The corresponding distribution of vertical velocities is shown in Fig. 10. To get the total vertical velocity the effect at lower levels should also have been considered. A rough calculation shows that these effects do not change the picture as a whole so that this can be taken as a crude approximation.

In Fig. 10 a few 24-hours trajectories are drawn. The 24-hours being from 0000 GMT February 21, to 0000 GMT February 22. At the point A advection alone should give a rise in temperature of 1° C. The observed change was —4° C. Corresponding values at B are 3° and 0° and at C —4° and —10° C. The effect of vertical motions must hence account for a decrease in temperature at A of —5°, at B of —3° and at C of —6° C. This does not agree too badly with the areas of ascending motion shown in Fig. 10, although the value at C seems rather high compared with the others. But one must remember the difficulties encountered in drawing the upper air charts even when previous and later charts are used for checking of the data. This is especially true when computing the absolute vorticity.

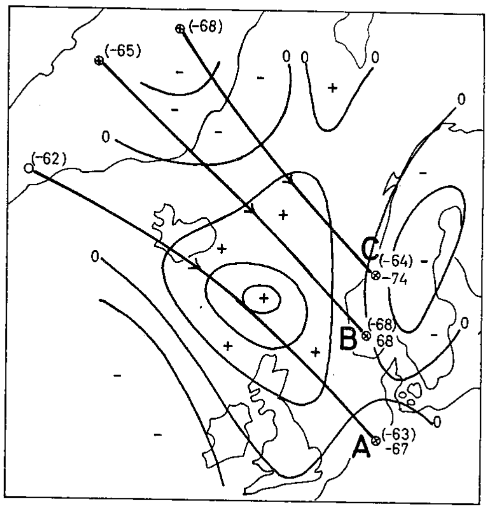

Fig. 10. Areas of ascending (+) and descending (÷) motions. Heavy curves: 24-hours trajectories. The numbers in brackets are observed temperatures at 0000 GMT, February 21. The other numbers are observed temperatures 0000 GMT, February 22, 1959.

The drop in temperature occurred mainly above the 100 millibar level in the region where the clouds were located. Unfortunately the observations are too scanty to apply the same method at any higher level. Anyway, a distribution of vorticity and thickness lines as shown schematically in Fig. 11 could quite well explain the region of low temperatures observed at the 50 millibar level as mainly being due to dynamic processes. The maximum cooling occurs where the thickness lines and the lines of equal absolute vorticity again become parallel. It is noteworthy that the vertical motions created will have a tendency to give the process a stationary character.

5.4 The soundings from Ørlandet give an opportunity to calculate the vertical velocity between the 70 and 50 millibar levels by applying the formula:

$$\omega = -\frac{\dfrac{\partial \omega}{\partial t} + \boldsymbol{v} \cdot \nabla_p \theta}{\dfrac{\partial \theta}{\partial p}}$$

where as before $\omega = \frac{Dp}{Dt}$ and θ = potential temperature. By use of the geostrophic wind equation the term $\boldsymbol{v} \cdot \nabla_p \theta$ is calculated by measuring the change of the wind with height and time. In this way the use of doubtful upper air charts may be avoided at points where direct measurements are available. It is assumed that an interval of 12 hours is not too long to give representative values of ω so that two successive radiosonde ascents can be used. The observed values of wind and temperatures at 0000GMT and 1200 GMT February 21 have been used. This gives a value of $\omega = -0.6$ cm/sec. That is an ascending motion of 21.6 meter/hour corresponding to an adiabatic cooling of 5.2° C in 24 hours. This method is not too reliable as the upper winds are not measured with the desired accuracy and the result is rather sensitive to small wind variations.

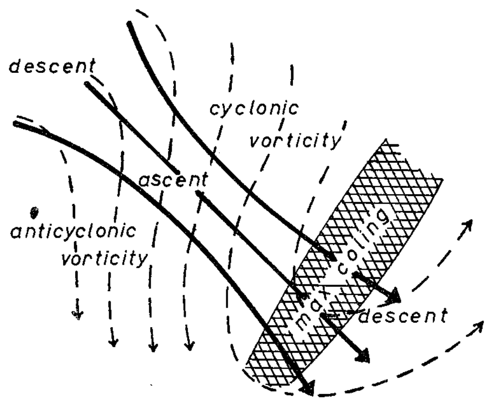

6. The influence of mountain waves.

6.1 There is little doubt that mountain waves really are necessary for mother of pearl clouds to occur. Palm and Foldvik [7] have studied the effect of waves and shown that a maximum displacement of the streamlines of 400 meter occurred at heights of 20 to 30 km in a case with mother of pearl clouds studied by Hesstvedt. From a theoretical point of view the case of February 21 is even more favourable for the formation of strong waves in the troposphere as well as in the stratosphere. It may be mentioned that on the following day waves with vertical velocities of 5 meter/sec. were observed by gliders over Drammen at heights between 2 and 3 km. The wavelength was 8 km. Due to lack of oxygen they could fly no higher. On February 21 the airstream was too turbulent at low levels to permit gliding. On February 22 the pilot of a Dakota plane reported weaker, but marked waves at 3 km extending from the south coast of Norway to Northern Denmark. The wavelength was 20 km.

6.2 In a recent work Eliassen and Palm [8] show that the energy originating from the mountains may be reflected from the atmosphere in such a manner that the shortest wavelength which may occur in the stratosphere may be estimated from the curve

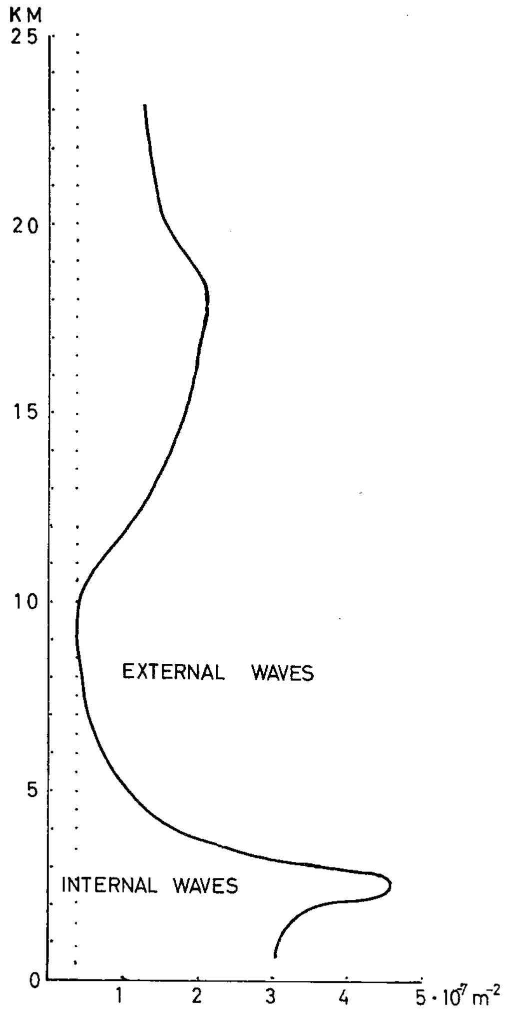

showing the distribution of a function $f(z)$. The shorter waves will be reflected from the upper troposphere and cannot penetrate into the stratosphere.

Here $f(z) = S/U^2 - Uzz/U$, where $S = g\ (\gamma_d - \gamma)/T$ measures static stability, g is the acceleration of gravity, γ_d the dry-adiabatic and γ the actual lapse rate, T the absolute temperature, U wind speed and Uzz the second derivative of U with respect to height.

Fig. 12 shows the distribution of $f(z)$ with height on February 21 at 1200 GMT. The curve is smoothed and the effect of the curvature term has been neglected. This does not appreciably affect the result. Only waves with wave numbers less than the minimum value $\sqrt{0.42 \times 10^{-7}\ \text{meter}^{-2}}$ can occur in the stratosphere. This gives a possible wavelength of about 30 km. Shorter wavelengths are not to be expected. Inspection of the pictures shows wavelengths of the order of 25 to 30 km to appear, together with longer waves of about 50 km. It is rather difficult from the photos and measurements to give definite values of wave amplitudes, but they seem to be of the order of 500 m, thus giving a cooling of 5° C of the ascending air. When assuming sinusoidal waves, with a windspeed of 60 meter/sec. and a wavelength of 30 km we get maximum vertical velicities of 5 meter/sec. With a wavelength of 50 km we get 3 meter/sec.

ACKNOWLEDGMENTS. The author is indebted to professor A. ELIASSEN and professor E. PALM for their valuable advice and comments. A special thank goes to Mr. O. SKOGVOLD of the Norwegian Meteorological Institute. Without his enthusiastic collaboration in collecting the photos and taking measurements this work could not have been done. Further I wish to thank Mr. W. HÅRVIG for drawing the figures.

REFERENCES.

1. DRIVING, A. YA and A. I. SMIRNOVA, 1958: *USSR Geophysical Series* No. 3. English Edition, translated and published by the American Geophysical Union, July 1959.
2. HESSTVEDT, E., 1959: *Geof. Publ.* **20**, No. 10.
3. — 1960: *Geof. Publ.* **21**, No. 9.
4. MURGATROYD, R. J., 1957: *Quart. J. R. Met. Soc.* **83**, p. 417.
5. ELIASSEN, A. and E. KLEINSCHMIDT, 1957: *Handbuch der Physik.* Band XLVIII, p. 97, Berlin—Göttingen—Heidelberg.
6. FJØRTOFT, R., 1955: Lectures (unpublished).
7. PALM, E. and A. FOLDVIK, 1960: *Geof. Publ.* **21**, No. 6.
8. ELIASSEN, A. and E. PALM, 1961: *Geof. Publ.*, **22**, No. 3.

Cloud A (Fig. 4) as seen from Holt 1615 GMT, February 21, 1959. Circles are drawn for angular distances of 10 and 15 degrees from the sun. (Photo: A. Holt).

Lier 1634 GMT. Cloud E (Fig. 4) with veil. The clouds C and D are seen just to the left of E. Cloud B is partly hidden behind low stratocumulus clouds. (Photo: Y. Gotaas).

Drammen 1644 GMT. The veil extending from cloud E (Fig. 4) is seen at the top of the picture. Cloud B with part of veil is in the center and to the left. (Photo: Y. Gotaas).

Stange 1645 GMT. Cloud B to the left and cloud E to the right. Both with veils (see Fig. 4). The clouds C and D are partly obscured by the head of the person standing on the right. (Photo H. G. Hemm).

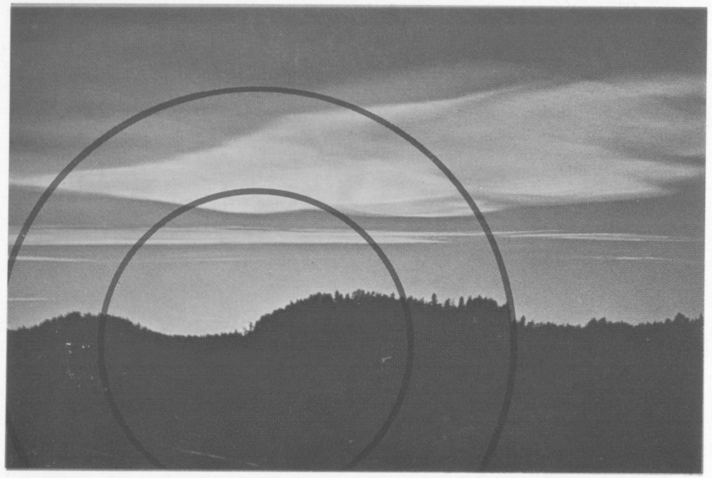

1 Holt Holt 1615 GMT

2 Lier 1634

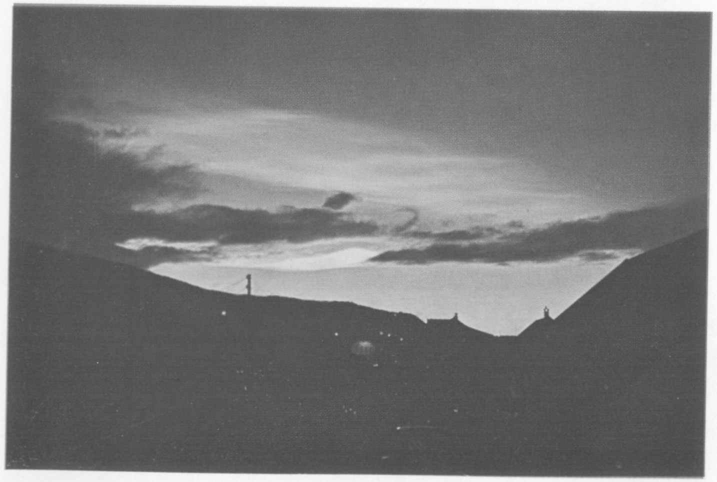

3 Drammen 1644 GMT

4 Stange 1645 GMT